NAVAL POSTGRADUATE SCHOOL
Monterey, California

THESIS

AEROSOL OPTICAL DEPTH RETRIEVAL WITH AVIRIS DATA: A TEST OF TAFKAA

By

James O. Rasure

September 2002

Thesis Advisor:	Philip A. Durkee
Second Reader:	Kurt Nielsen

Approved for public release; distribution is unlimited.

THIS PAGE INTENTIONALLY LEFT BLANK

REPORT DOCUMENTATION PAGE

Form Approved OMB No. 0704-0188

1. AGENCY USE ONLY *(Leave blank)*	2. REPORT DATE	3. REPORT TYPE AND DATES COVERED
	September 2002	Master's Thesis

4. TITLE AND SUBTITLE: Aerosol Optical Depth Retrieval With AVIRIS Data: A Test Of Tafkaa

5. FUNDING NUMBERS

6. AUTHOR(S) Rasure, James O.

7. PERFORMING ORGANIZATION NAME(S) AND ADDRESS(ES)
Naval Postgraduate School
Monterey, CA 93943-5000

8. PERFORMING ORGANIZATION REPORT NUMBER

9. SPONSORING / MONITORING AGENCY NAME(S) AND ADDRESS(ES)

10. SPONSORING / MONITORING AGENCY REPORT NUMBER

11. SUPPLEMENTARY NOTES: The views expressed in this thesis are those of the author and do not reflect the official policy or position of the Department of Defense or the U.S. Government.

12a. DISTRIBUTION / AVAILABILITY STATEMENT
Approved for public release; distribution unlimited.

12b. DISTRIBUTION CODE

13. ABSTRACT ***(maximum 200 words)***

Using solar wavelength radiance data obtained from the airborne AVIRIS instrument, during the LEO experiment, an analysis of aerosol optical depth (AOD) was completed using Tafkaa - a program developed by the Naval Research Laboratory (NRL). The objective of the analysis was to compare Tafkaa-retrieved AOD with AOD retrieved from SeaWiFS, and ground-based sun photometers. The intent of the study was to test enhanced AOD analysis using the hyperspectral coverage provided by AVIRIS. Comparisons between AOD retrieved by Tafkaa provided results consistent with SeaWiFS AOD retrieval and the AOD determined by ground-based sunphotometers in regions with minimal sediment and sun glint. A reliable sun glint mask was produced and applied to remove the effects of sun glint in the AVIRIS data.

14. SUBJECT TERMS: AVIRIS, Aerosol Optical Depth, AOD, LEO, Tafkaa

15. NUMBER OF PAGES 57

16. PRICE CODE

17. SECURITY CLASSIFICATION OF REPORT	18. SECURITY CLASSIFICATION OF THIS PAGE	19. SECURITY CLASSIFI- CATION OF ABSTRACT	20. LIMITATION OF ABSTRACT
Unclassified	Unclassified	Unclassified	UL

NSN 7540-01-280-5500

Standard Form 298 (Rev. 2-89)
Prescribed by ANSI Std. 239-18

THIS PAGE INTENTIONALLY LEFT BLANK

Approved for public release; distribution is unlimited

AEROSOL OPTICAL DEPTH RETRIEVAL WITH AVIRIS DATA: A TEST OF TAFKAA

James O. Rasure
Lieutenant Commander, United States Navy
B.S., University of Evansville, 1988

Submitted in partial fulfillment of the
requirements for the degree of

MASTER OF SCIENCE IN METEOROLOGY AND PHYSICAL OCEANOGRAPHY

from the

NAVAL POSTGRADUATE SCHOOL
September 2002

Author:

James O. Rasure

Approved by:

Philip A. Durkee, Thesis Advisor

Kurt E. Nielsen, Second Reader

Carlyle H. Wash, Chairman
Department of Meteorology

THIS PAGE INTENTIONALLY LEFT BLANK

ABSTRACT

Using solar wavelength radiance data obtained from the airborne AVIRIS instrument, during the LEO experiment, an analysis of aerosol optical depth (AOD) was completed using Tafkaa - a program developed by the Naval Research Laboratory (NRL). The objective of the analysis was to compare Tafkaa-retrieved AOD with AOD retrieved from SeaWiFS, and ground-based sun photometers. The intent of the study was to test enhanced AOD analysis using the hyperspectral coverage provided by AVIRIS. Comparisons between AOD retrieved by Tafkaa provided results consistent with SeaWiFS AOD retrieval and the AOD determined by ground-based sunphotometers in regions with minimal sediment and sun glint. A reliable sun glint mask was produced and applied to remove the effects of sun glint in the AVIRIS data.

THIS PAGE INTENTIONALLY LEFT BLANK

TABLE OF CONTENTS

THIS PAGE INTENTIONALLY LEFT BLANK

LIST OF FIGURES

LIST OF TABLES

THIS PAGE INTENTIONALLY LEFT BLANK

ACKNOWLEDGEMENTS

I would like to thank my advisor, Dr. Philip A. Durkee of the Department of Meteorology, Naval Postgraduate School, for his guidance and support during the development of this thesis. Additionally, I would like to thank Mr. Kurt Nielsen of the NPS Remote Sensing Laboratory for his support with SeaWiFS data acquisition and for his support as second reader.

I also thank Dr. Marcos Montes, Dr. William Snyder, and Dr. Curt Davis from the Remote Sensing Division, Naval Research Laboratory, Washington, DC for their help in obtaining the AVIRIS data and for providing the Tafkaa software.

THIS PAGE INTENTIONALLY LEFT BLANK

I. INTRODUCTION

A. MOTIVATION

Atmospheric aerosol particles affect the global climate, reduce horizontal visibility, and interfere with electromagnetic propagation. An accurate understanding of the structure and composition of atmospheric aerosols is extremely important in understanding the Earth's radiation budget. According to Charlson et al. (1992) and the international Panel on Climate Change (IPCC) (1996), the effects of atmospheric aerosols may work to offset the greenhouse warming effect measurably. This is accomplished by at least two mechanisms. First, the increased scattering of incoming solar radiation, as it encounters atmospheric aerosol particles, increases the amount of solar energy that is reflected back into space. Secondly, increased aerosol concentration provides additional condensation nuclei, which in turn increases the cloud albedo at solar wavelengths.

Any remotely obtained image at solar wavelengths is contaminated by the aerosols in the air column between the sensor and the surface of the Earth. The absorption and scattering effects produced by these atmospheric aerosols distort information about the surface. In order to extract usable information from remotely sensed imagery, the images must be corrected for this atmospheric contamination. Application of accurate atmospheric corrections to remotely sensed images is an important first step in obtaining useful information. The most important parameter to understand to develop an accurate atmospheric correction is the Aerosol Optical Depth (AOD). The Aerosol Optical Depth is defined as an index of the attenuation of radiation as it passes through the atmosphere due to the suspended particles (Angstrom 1964). It can be calculated by summing the scattering potential over the aerosol size distribution

B. AOD MEASUREMENT

The AErosol RObotic NETwork (AERONET) is an international network of ground-based sunphotometers. This collection of over one hundred individual sunphotometers covers a large portion of the Earth's land surface. In conjunction with other networks, AERONET sites are used to study aerosol processes and validate satellite data. The small number of nodes limits the spatial resolution. Clearly there is a need for a method of AOD retrieval that can cover more of the globe in a timely manner.

Collection from space yields broader spatial coverage than the network of ground-based sunphotometers, depending on orbit parameters. Space-based sensors provide a near global coverage that is repeated at regular intervals. The current space-based sensors are primarily multispectral in design. Multispectral sensors collect images in a discrete number of broad wavelength bands. When Landsat 1 was launched in 1972, multispectral imaging was the new revolution. The Sea-viewing Wide Field of view Sensor (SeaWiFS) is one of the current multispectral sensors in operation. Launched onboard the SeaStar spacecraft on 1 August 1997, SeaWiFS provides multispectral images of the Earth's surface utilizing 8 wavelength bands ranging from 412nm to 865nm. Bands 6 (670 nm), 7 (760 nm), and 8 (865 nm) are used to determine atmospheric aerosol properties.

Multispectral imagers lack sufficient spectral resolution for some scientific applications. The future of remote sensing is in the ability to collect and interpret hyperspectral imagery. Hyperspectral imagery, in contrast to multispectral imagery, measures incoming radiation in a large number of narrow wavelength bands. Due to the large number of contiguous bands, hyperspectral imagery has the potential to provide scientists with the ability to extract more information from the data at an accuracy that greatly exceeds multispectral applications.

Hyperspectral sensors are instruments much like laboratory spectrometers. The incoming radiation is split into many discrete wavelengths. Hyperspectral instruments have been operated primarily on airborne platforms. However, with the advent of NASA's Hyperion sensor on EO-1 and the U.S. Air Force Research Lab's FTHSI sensor on the MightySat II, hyperspectral sensors will become the space-based sensor of the future. Of paramount importance is the ability to atmospherically correct these images. The Naval Research Laboratory (NRL) has developed software to be used to obtain ocean color properties from the Hyperion data. This program will be tested on AVIRIS data prior to Hyperion becoming operational.

Hyperion, like AVIRIS is a hyperspectral sensor covering the range of wavelengths from 400 nm to 2500 nm. Hyperion uses 220 bands where AVIRIS utilizes 224 bands. Hyperion produces a 7.5 km by 100 km image at 30 m resolution. Some

applications for these new hyperspectral images include: Biomass burning studies, Coastal and Inland Studies, Ecology, Environmental Hazards, Geology, Satellite Calibration, Snow and Ice Studies, and Vegetation Studies.

C. OBJECTIVE

Remotely collected imagery from AVIRIS can be used to provide ocean color analysis. In order to extract usable data from an image, an atmospheric correction algorithm must be applied to a raw image. The objective of this thesis is to compare the AOD retrievals obtained from Tafkaa, developed by the Naval Research Laboratory (NRL), with AOD retrievals from SeaWiFS data using SeaDAS. SeaDAS (SeaWiFS Data Analysis System) is a comprehensive image analysis package developed by NASA for processing, displaying and analyzing all SeaWiFS (Sea-viewing Wide Field-of-view Sensor) data products and ancillary data. The utility of the atmospheric correction included in the Tafkaa software developed by NRL as it is applied to the hyperspectral images collected by AVIRIS will be evaluated as it compares to the SeaDAS-generated AOD retrievals and the ground-based sunphotometer data.

D. ORGANIZATION

Chapter II provides some review of the basic radiative transfer theory as well as background information on the Long Term Ecosystem Observatory (LEO) site, the AVIRIS sensor and the two primary computer programs utilized to analyze the AVIRIS data (Tafkaa and MASK), the SeaWiFS sensor and the accompanying computer software SeaDAS, and AERONET sunphotometers. Chapter III describes the methodology of using MASK and Tafkaa for atmospheric correction and AOD retrieval from AVIRIS data as well as how SeaDAS was employed on the SeaWiFS data. Chapter IV outlines the results and comparisons. Finally, chapter V presents the conclusions of this thesis and offers recommendations for further studies.

THIS PAGE INTENTIONALLY LEFT BLANK

II. BACKGROUND INFORMATION

This chapter will provide some useful background information on basic radiative transfer theory. Also included in this chapter is a description of the data collection site and the three sensors used in this study (AVIRIS, SeaWiFS, and sunphotometers). Also briefly described in this chapter are the two primary atmospheric correction algorithms used in this study (Tafkaa and SeaDAS).

A. BASIC RADIATIVE TRANSFER THEORY

A basic understanding of radiative transfer theory and the Radiative Transfer Equation (RTE) is of particular importance when studying the measurement of atmospheric properties from space. For a complete explanation of radiative transfer theory see Liou, 1980.

Figure 1 is a graphic depiction of the basic elements of the RTE. The radiance measured by remote sensors such as AVIRIS and SeaWiFS is the result of several sources including: Rayleigh (molecular) scattering, surface reflectance, sun glint, and Mie (aerosol) scattering of incoming solar photons from the air column. In order to isolate the radiance due only to the aerosols, all other sources must be removed. The Radiative Transfer Equation (RTE) was developed in order to mathematically quantify these sources and sinks of atmospheric radiation. Through a variety of assumptions, the RTE can be reduced to a more usable form. When dealing with atmospheric aerosols, for relatively low AOD, radiance sources can be accounted for in the following linear expression (Gordon and Clark, 1980): $L_t = L_a + L_r + (L_s + L_g)?$, where L_t is the total radiance received at the sensor, L_a is the aerosol radiance, L_r is the radiance due to Rayleigh scattering, L_s is the surface-reflected radiance, L_g is the sun glint radiance due to specular reflectance, and ? is the transmittance of the atmosphere. The surface reflected radiance (L_s) is minimal beyond 750 nm for areas that are free from surface and sub-surface contaminants such as sea foam and sediment. An area where L_g (sun glint) is present, specular reflectance masks the desired radiance measurements. These areas can be avoided by geometry considerations.

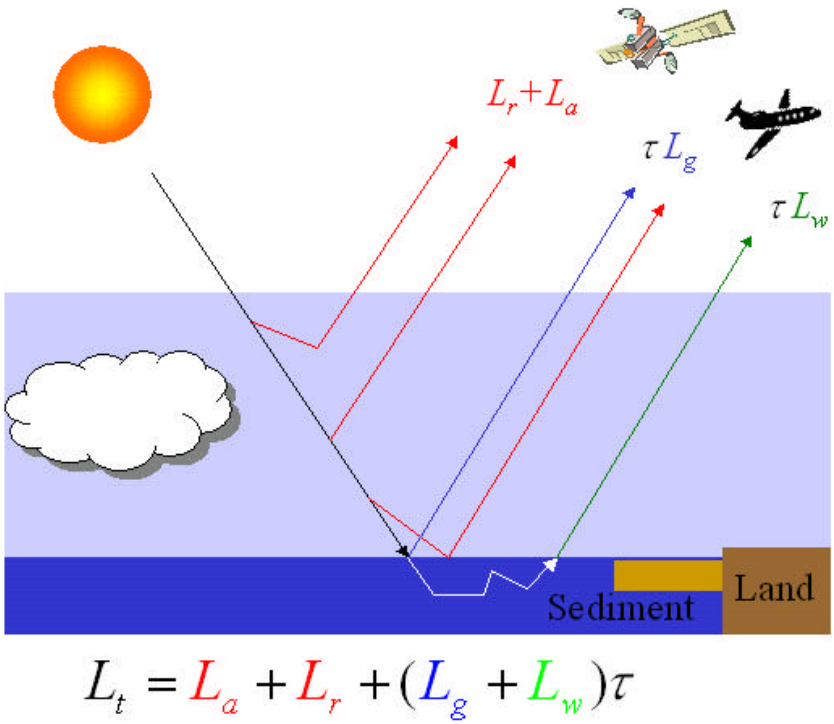

Figure 1. Illustration of the various terms in the radiative transfer equation where L_t is total radiance at sensor, L_w is the water leaving radiance, L_g is the sun glint, $L_r + L_a$ are the Rayleigh scattering and aerosol radiance respectively, and ? is the transmittance of the atmosphere.

Although wavelength is a major consideration in determining the scattering phase function, the size distribution and composition of the atmospheric aerosols play a major role in determining the scattering phase function. Mie theory describes the scattering phase function when interactions are between particles and radiation whose wavelengths are nearly the same as that of the particles circumference. In order to accurately quantify the phase function in Mie scattering, an understanding of the aerosol composition and size distribution must be known. Shettle and Fenn (1979) incorporated a phase function using measured averaged size distributions and characteristics for a region to parameterize this phase function. The size distributions of Shettle and Fenn (1979) are used by Tafkaa and SeaDAS and are described later in this document.

B. LONG-TERM ECOSYSTEM OBSERVATORY (LEO) SITE

Figure 2 shows the Long Term Ecosystem Observatory site and many of the sensors that were deployed for the 2000 - 2001 experiments. The LEO site is located in

the New York Bight off the coast of New Jersey, USA. This location has been developed and operated for the main purpose of developing real-time environmental assessments. Environmental data is collected from satellites, aircraft, ships, fixed/movable moorings and autonomous underwater vehicles. The observatory system has been in operation since 1998 and has been home to four annual coastal predictive skill experiments.

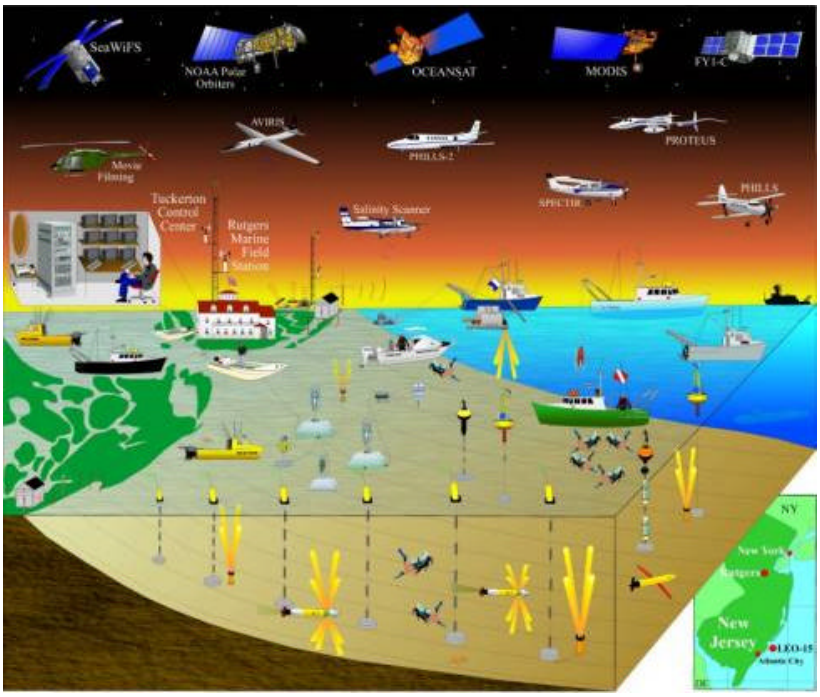

Figure 2. Depiction of the LEO site and instrumentation used for the 200-2001 experiment.

C. AIRBORNE VISIBLE/INFRARED IMAGING SPECTROMETER (AVIRIS)

AVIRIS was just one of many instruments used to collect data at the LEO site in 2000-2001. The AVIRIS instrument is an airborne hyperspectral imaging instrument capable of collecting data in 224 contiguous, 10 nm wide bands that cover the entire range of wavelengths from 410 nm to 2450 nm. Figure 3 shows the AVIRIS, SeaWiFS, and the sunphotometer spectral coverage superimposed on the curves of atmospheric transmission and solar irradiance. AVIRIS uses a nadir viewing whiskbroom scanner over a 30-degree field of view to record data in 614 pixels for each of the 224 bands. The spatial response of 1.0 mrad corresponds to a pixel size of 20 m by 20 m for high altitude

flights and 4 m by 4 m for low altitude heights. The data are collected in scenes of 512 scan lines supplying an image along the flight path approximately 11 km wide for high altitude flights. Figure 4 is a typical AVIRIS image rendered in true color. This image was produced using band 35 (673 nm) for red, band 19 (548 nm) for green, and band 8 (441 nm) for blue.

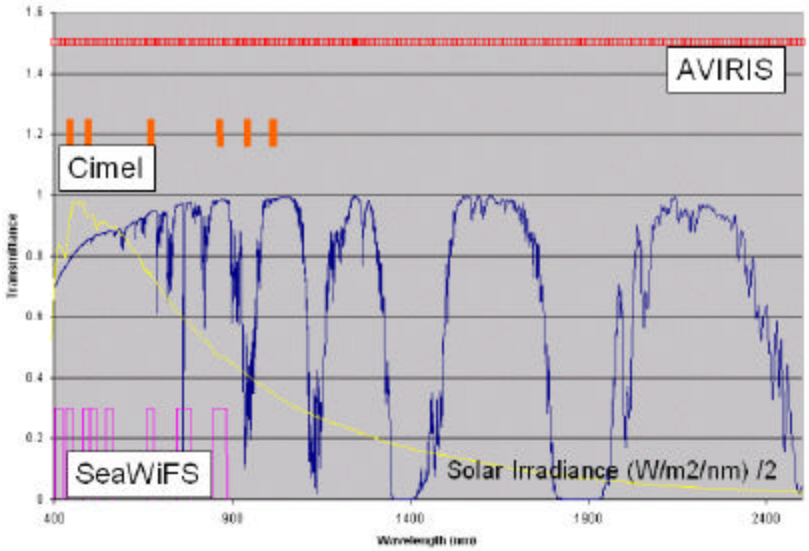

Figure 3. AVIRIS, SeaWiFS, and Cimel sunphotometer spectral coverages superimposed on the transmission curve and the solar irradiance curve.

The best method of representing a set of hyperspectral data such as AVIRIS is by using a data cube with two axes for the spatial dimensions and the third axis representing the 224 channels that make up the spectral dimension. Figure 5 is an "image cube" from AVIRIS that shows the volume of data returned by the instrument. AVIRIS acquired the data on August 20, 1992 when it was flown on a NASA ER-2 plane at an altitude of 20 km over Moffet Field, CA, at the southern end of San Francisco Bay. (AVIRIS Home Page)

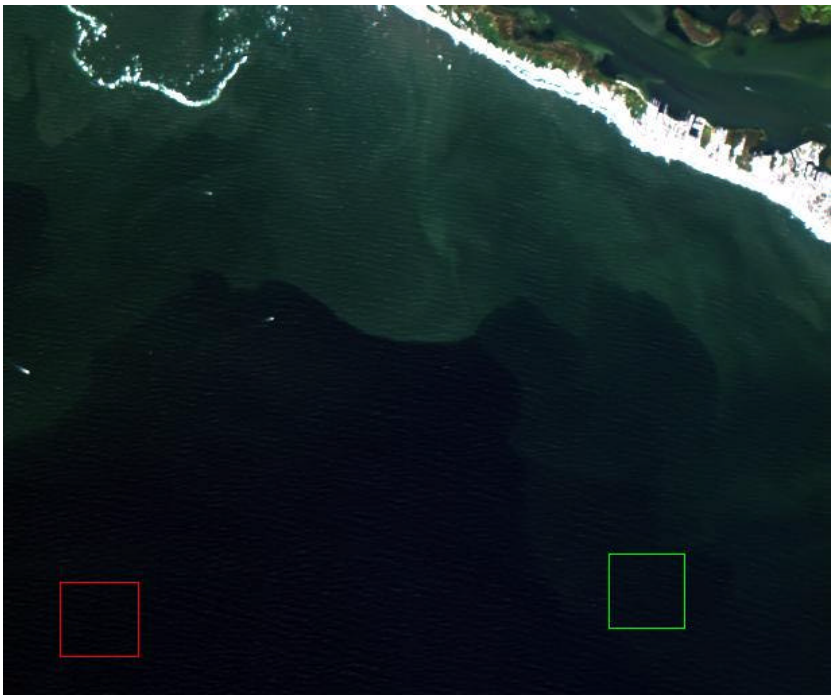

Figure 4. July 31, 2001 AVIRIS scene 5 rendered in true color using band 35 (673 nm) for red; band 19 (548 nm) for green, and band 8 (441 nm) for blue.

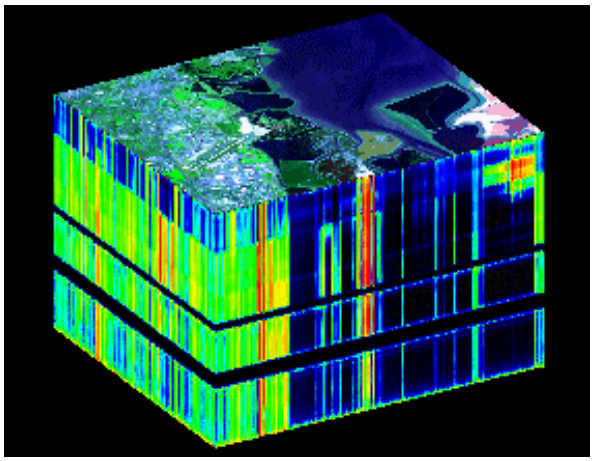

Figure 5. Data cube acquired by AVIRIS on August 20, 1992 when it was flown on a NASA ER-2 plane at an altitude of 20 km over Moffet Field, CA, at the southern end of San Francisco Bay.

Each individual AVIRIS pixel from an average image contains a radiometrically corrected spectrum usually expressed in radiance. AVIRIS radiance measurements are reported in units of mW cm^{-2} nm^{-1} sr^{-1}. AVIRIS radiometric calibration factors are

calculated by measuring the response of AVIRIS to an integrating sphere (a known target illuminated by a known light source). This calibration is accurate to within 7%, absolute over time. Intra-flight accuracy is within 2%. Figure 6 shows a typical spectral profile of AVIRIS data collected over water.

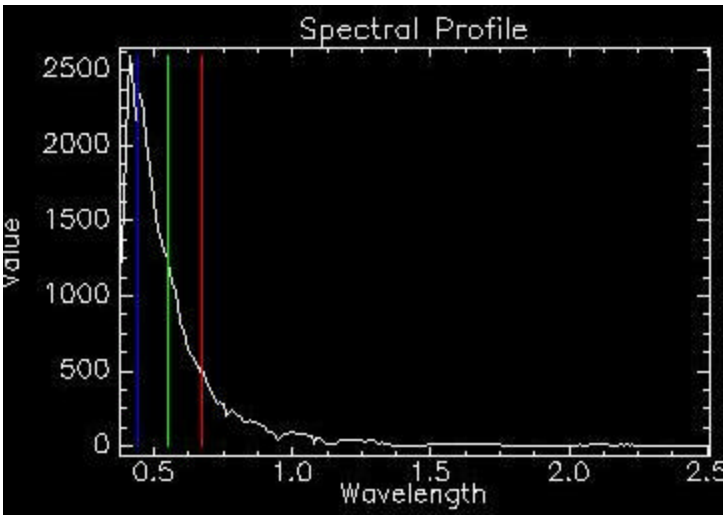

Figure 6 Over water Spectral Reflectance extracted from AVIRIS data. ENVI, the Environment for Visualizing Images produced this chart of AVIRIS data collected on July 12, 1998.

D. TAFKAA

Tafkaa is an algorithm developed at the Naval Research Laboratory (NRL) (Montes 2002) in an attempt to atmospherically correct hyperspectral imagery for remote sensing of ocean color with the future hyperspectral HYPERION sensor. Tafkaa utilizes a spectrum-matching technique to derive information on the atmospheric aerosols present in an image cube. The similarity in data sets acquired via HYPERION and AVIRIS allows for the testing of the Tafkaa codes on AVIRIS data in preparation to the acquisition of the HYPRERION data sets.

Tafkaa calculates the reflectance due to atmospheric scattering, and direct sunlight and diffuse skylight reflection off of the rough ocean surface, the upward transmission due to scattering, the downward transmittance through the atmosphere to the target, the average reflectivity at the base of the atmosphere, and the transmission due to

the absorptive processes in the gas. These quantities are tabulated utilizing a modified version of the Ahmad and Fraser (1982) code. This code was chosen by NRL for inclusion in the Tafkaa algorithm because of the proper atmospheric layering structure and the treatment of the wind roughened water surfaces. Tafkaa allows the user to select the wind speed according to the weather conditions at the time of the data collection.

In order to determine the pressure and water vapor mixing ratios at the various heights in the atmosphere, Tafkaa allows the user to select which atmospheric model is to be used. The choices are: Mid-Lat Summer, Mid-Lat Winter, Tropical, Sub Arctic Summer, Sub Arctic Winter, and US Standard 1962. The data were collected during Mid-Lat Summer therefore, this selection was chosen for the analysis described here.

Different sets of gases present in the atmosphere require different treatments. Tafkaa allows the user to select or deselect which of these gases are thought to be present in significant concentrations in the air column. The choices are: H_2O, CO_2, O_3, CO, N_2O, CH_4, NO_2 and O_2. The absorptive coefficients for H_2O, CO_2, N_2O, CO, CH_4 and O_2 are accounted for by using files that are stored in the Tafkaa data directory. Each file contains 300,000 spectral locations and 19 atmospheric layers. These files are based on a line-by-line code developed by W. Ridgeway at NASA Goddard Space Flight Center (Montes 2002). The spectral resolution is 0.05 cm^{-1} in the range 560 - 3100 nm. The coefficients for O_3 were derived from LOWTRAN7 O_3 transmittance spectra calculated with the US76 atmospheric model. Tafkaa assumes that ozone is in an infinitesimal layer at 27 km. No errors were introduced by this assumption since the sensor was flown well below this layer.

The radiance scattered by the aerosol particles in the air column must be measured to determine the AOD. This requires the use of a very powerful assumption, the dark water assumption. This assumption states that there is no water leaving radiance at wavelengths longer than about 750 nm due to the strong absorption of light by water. Therefore, in truly dark water, the only radiance reaching the sensor is that which is scattered by the aerosols in the air column. The presence of clouds, land, sun glint and sediments are factors that invalidate the dark water assumption. Clouds contaminate the AOD retrieval due to radiance at all wavelengths. Masking algorithms are available that

mask clouds by recognizing their spectral signatures. The spectral resolution of the AVIRIS data allows for more reliable cloud masks. Land is similarly masked. Sediments, on the other hand, are not so easily masked due to the wide variety of types and consequently the varied spectrum produced by them. Sediments in the water scatter energy at the shorter wavelengths thereby rendering the dark water assumption invalid.

Another factor that affects the dark water assumption is the presence of sun glint. Sun glint is energy specularly reflected back to the sensor from the surface. This energy is distributed in all wavelengths of the solar spectrum (see Figure 7). Figure 7 is a graph of the incoming solar radiation. The best method for dealing with sun glint is to avoid it. The dark water assumption generally holds well for scenes in deep, smooth water off the coast, free of sediments and suspended particles and away from sun glint geometry.

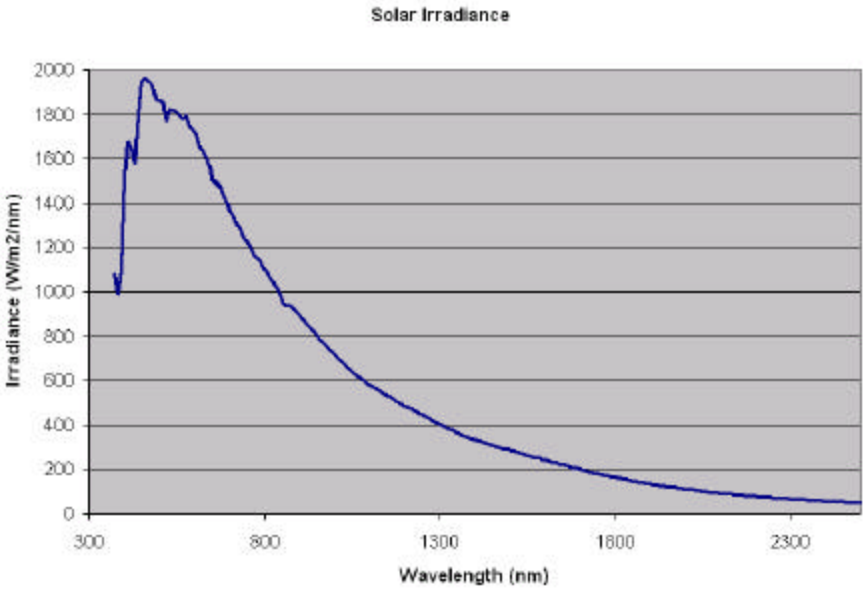

Figure 7. Typical blackbody curve for incoming solar radiation.

SeaWiFS only has two wavelength bands available longer than the 750 nm dark water assumption and SeaDAS uses two wavelengths for AOD retrieval (670 nm and 860 nm). The 670 nm band is shorter than the dark water assumption. AVIRIS, on the other hand collects data in many bands longer than the 750 nm dark water assumption. Tafkaa offers the user the ability to determine which wavelengths are used in the AOD retrieval.

Table 1 is a list of all wavelengths that can be chosen within Tafkaa for this determination. Table 2 lists the various wavelengths chosen in Tafkaa for AOD retrieval used in this thesis. Combination A, 670 nm and 860 nm, compares to the wavelengths used in the SeaDAS AOD retrievals. Combination B is the combination of wavelengths utilized by NRL during ocean color analysis of AVIRIS data. This combination uses wavelengths above 750 nm. Combination C is the NRL combination with the 670 nm wavelength added to aid in the retrievals in sediment regions. The various windows in the atmospheric transmission curve (Figure 3) determined which wavelengths were available to Tafkaa.

Table 1 Tafkaa AOD Wavelengths

Wavelength (nm)	Wavelength (nm)
390	410
440	470
510	550
610	670
750	870
1020	104
1240	164
2250	

Table 2 Wavelength Combinations

Id	Description	Wavelengths (nm)
A	SeaWiFS-like	670, 860
B	NRL Wavelengths	750, 860, 1040, 1240, 1640, 2250
C	A + B	670, 750, 860, 1040, 1240, 1640, 2250

E. SEA-VIEWING WIDE FIELD OF VIEW SENSOR (SEAWIFS) AND SEAWIFS DATA ANALYSIS SYSTEM (SEADAS)

SeaWiFS was launched to low earth orbit on August 1, 1997 as part of the SeaStar spacecraft developed by OSC. SeaWiFS is a multi spectral instrument that collects data in 8 separate wavelength bands from 402 nm to 885 nm. The first six bands have a bandwidth of 20 nm while the last two have a band width of 40 nm. Table 3 provides a comparison between the AVIRIS instrument and the SeaWiFS instrument. The larger number of bands and the narrower bandwidth provide a much larger spectral coverage for AVIRIS. The 12-bit digitization gives AVIRIS more spectral resolution than the 10-bit digitization of the SeaWiFS instrument. The SeaWiFS instrument may be tilted forward or backward 20 degrees along the spacecraft orbital trajectory to minimize the effects of sun glint (From SeaWiFS homepage) while no such adjustment s are made with AVIRIS' downward pointing sensor. The pixel size and swath width provide much improved spatial resolution that allows for analysis to be performed on individual pixels that are free of sun glint.

Table 3 Comparison of AVIRIS to SeaWiFS sensors

	AVIRIS	SeaWiFS
Bands	224 (374-2507 nm)	8 (412-865 nm)
Bandwidth	10 nm	20 nm
Pixel Size	20m X 20m	1.1 - 4.5 km
Swath Width	11 km	1502-2801 km
Digitization	12-bit	10-bit
Software	IDL ENVI Tafkaa	SeaDAS

The computer software SeaDAS, which is a comprehensive image analysis package for the processing, display, analysis, and quality control of all SeaWiFS data, was used in this study. (From SeaDAS homepage) SeaDAS utilizes lookup tables in much the same manner as Tafkaa's spectral matching technique.

F. AEROSOL ROBOTIC NETWORK (AERONET)

Each AERONET site utilizes a Cimel Electronique CE 318-1 standard sunphotometer. This is an all-weather instrument that is robotically pointed skyward. This radiometer takes two measurements, a direct sun shot and a sky shot. Each of these images is made within several programmed sequences. The direct sun measurements are made in eight separate bands (340, 380, 440, 500, 670, 870, 940, 1020 nm). The 940 nm band is used for a water column measurement. Optical depth is calculated from the spectral extinction of the direct beam for each of the eight wavelengths based on the Beer-Bouguer Law. (From http://aeronet.gsfc.nasa.gov:8080/)

THIS PAGE INTENTIONALLY LEFT BLANK

III. DATA AND PROCEDURES

Reference data were collected utilizing the AVIRIS instrument over the LEO site during two separate experiments. This data were used to validate the AOD retrieval from hyperspectral data using Tafkaa. The first collection occurred on July 12, 1998 while the second occurred on July 31, 2001. SeaWiFS data were obtained for the same area at approximately the same time in order to make direct comparisons of AOD retrievals. Data collected via the AERONET sunphotometer located at Brookhaven (1998) and Goddard Institute of Space Studies (GISS) (2001) were also used for comparison. This chapter will briefly describe the applicable weather conditions as well as the data sets and procedures used for this study.

A. WEATHER AT LEO

The most important weather parameters for this study were cloud cover and wind speed. Areas obscured by cloud cover do not provide useful information for the AOD retrieval due to the high reflectivity of the clouds in the visible portion of the spectrum. The wind speed is directly related to the roughness of the ocean and consequently, the amount of sun glint that will hinder the atmospheric correction algorithms. The first data set was obtained on July 12, 1998 at 14:03 GMT. The weather conditions as reported from weather station 44025 Long Island (closest to the collection site) from 1300 GMT to 1500 GMT were as follows: Winds were from 301 to 327 at 2.1 - 5.1 kts gusting to 2.7 - 5.9 kts. Wave height was .5 to .58 m. Water temperature was near 21 ^{o}C and air temperature was near 20 ^{o}C. Figure 8 is a SeaWiFS image collected at 1801 on July 12, 1998. This image clearly shows that for the date and time being studied, the area of concern is relatively cloud free with the exception of the diagonal cloud band in scene 4. This cloud band was easily masked prior to Tafkaa employment. Figure 9 is an AVIRIS image of the same area that also shows a relatively cloud-free day.

The second data set was obtained on July 31, 2001 at 14:16 GMT. The weather conditions as reported from weather station 44025 Long Island (closest to the collection site) from 1300 GMT to 1500 GMT were as follows: Winds were from 160 to 330 at 4.3 - 6.7 kts gusting to 5.1 - 7.7 kts. Wave height was 1.6 to 1.8 meters. Water temperature was near 20 ^{o}C and air temperature was near 19 ^{o}C. Figure 10 is a SeaWiFS image

collected at approximately 1753 on July 31, 2001. This image clearly shows that for the date and time being studied, the area of concern is relatively cloud-free. Figure 11 is an AVIRIS image of the same area that also indicates a relatively cloud-free day.

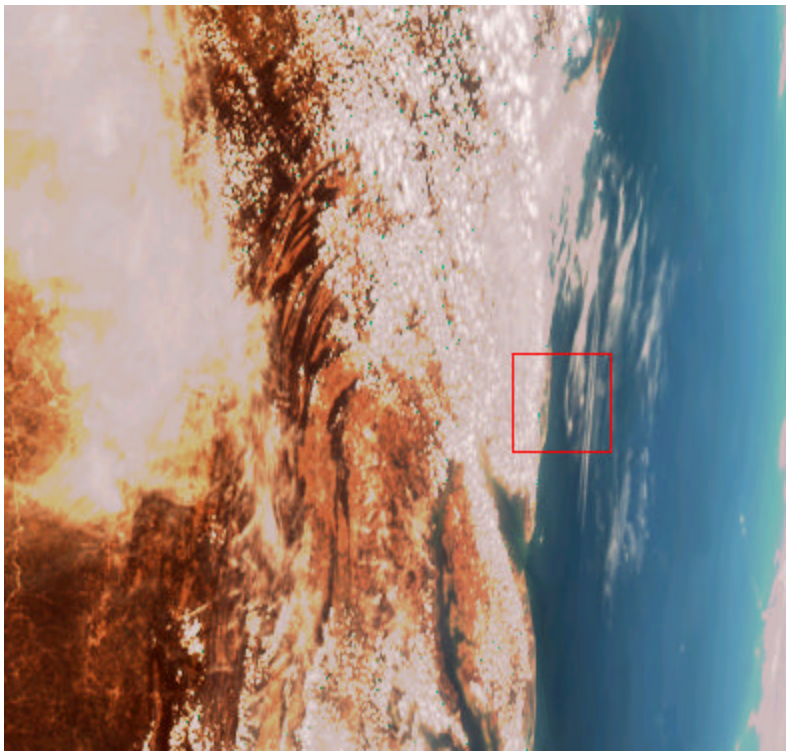

Figure 8 True color SeaWiFS image for July 12, 1998

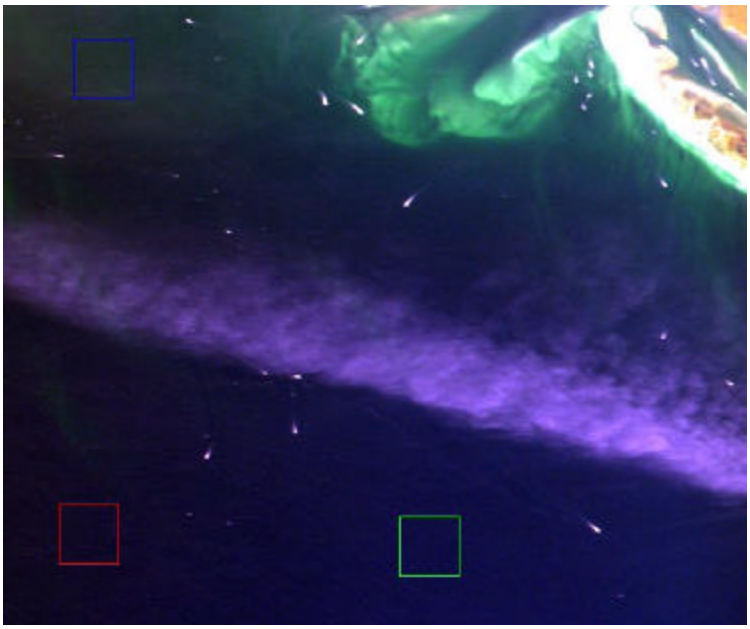

Figure 9. AVIRIS data collected at the LEO site on July 12, 1998. This is scene 4 of the complete data set.

Figure 10 True color SeaWiFS image for July 31, 2001

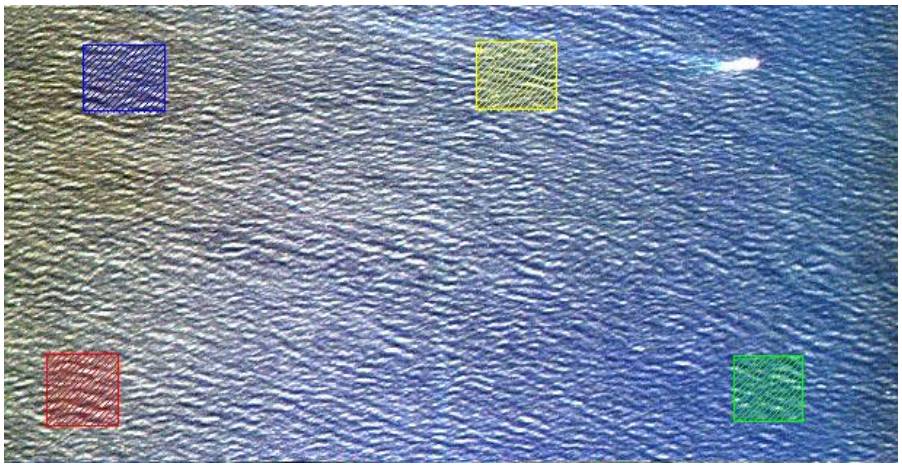

Figure 11. AVIRIS data collected at the LEO site on July 31, 2001. This is scene 11 of the complete data set.

B. AVIRIS DATA COLLECTION

The AVIRIS data for both days in this study, July 12, 1998 and July 31, 2001, were collected by the AVIRIS instrument as it was flown on NASA's ER-2 aircraft at a nominal altitude of 20 km and a nominal speed of 734 km/hr. This altitude and speed closely resembles a space borne sensor such as the Hyperion instrument.

The 1998 data are presented in two separate scenes. Note the turbid coastal water as well as the cloud feature in scene 4 in Figure 9. The 2001 data collection started over land at 39 33 11 N, 074 38 23 W at 14:09 GMT and ended over deep water at 32 25 21 N, 073 39 5 W at 14:16 GMT. Scenes 1 through 4 were primarily land or estuary and were not analyzed in this study. Figure 4 shows the true color image of scene 5 of the 2001 data set. This scene contained sediment in the upper left hand corner of the image that affected the shape of the AOD spectral variation curves. Scenes 6 through 11 covering an area approximately 11 km wide by 55 km long were the most useful in this study. Figure 11 shows scene 11 of the 2001 data set and was the most useful open water scene for this study.

Small areas within each AVIRIS scene, referred to as Regions of Interest (ROI), were selected for detailed analysis. The following Region of Interest (ROI) color scheme

applies to all figures in this document: ROI 1 (red), ROI 2 (green), ROI 3 (blue) ROI 4 (Yellow), ROI 5 (Cyan)

C. AOD RETRIEVAL FROM AVIRIS DATA

Tafkaa generates a *products* file that contains data "layers" that include estimates of column water vapor concentration and AOD at 550 nm, and the aerosol model and relative humidity selected to estimate AOD. The operator is given a variety of choices each time Tafkaa is employed on a scene. It is the purpose of this thesis to examine various combinations of selections and compare the Tafkaa-derived AOD's to the AOD's retrieved from SeaWiFS/SeaDAS, SeaWiFS/NPS model, and the AERONET sunphotometer AOD's. This section outlines the basic procedures for determining the AOD from the AVIRIS images.

1. MASK

NRL developed a simple program titled MASK that was used to mask out scene properties that hinder accurate AOD retrieval. The four masks created by this program mask out bad pixels, low altitude clouds, cirrus clouds, and land. As stated in the users guide for MASK, the land mask is the most robust of the four. The low altitude cloud and the cirrus cloud masks are in the process of being improved by NRL. The land mask option allows the user to choose one of two possible masking methods. The first is a Normalized Difference Vegetative Index (NDVI) and the second is a simple reflectance limit at a specified wavelength.

The NDVI is a good discriminator between land and water when the land has significant vegetation coverage. NDVI is defined as:

$$NDVI \equiv \frac{r_{obs}(0.86mm) - r_{obs}(0.66mm)}{r_{obs}(0.86mm) + r_{obs}(0.66mm)}$$

Where,

$$r_{obs}(l) \equiv \frac{pL_t}{m_o E_o}$$

r_{obs} = observed reflectance

l = wavelength

L_t = observed radiance

$m_o = \cos q_o$

q_o = solar zenith angle

E_o = extraterrestrial solar irradiance

Over water, NDVI is usually a negative value. Therefore, it is safe to state that NDVI > 0.05 implies "land".

The reflectance limit land mask simply allows the user to select a wavelength and a radiance limit that determines "land". The reflectance limit mask is used to mask out "trouble" pixels as well as land. This option was used in this thesis in order to mask out sun glint. It is possible that when a reflectance limit is set, it does not remain consistent for the entire data set. Therefore, the NDVI is a much more consistent identifier of land.

MASK set up with the NRL defaults was used on the 1998 data set to provide land masks and low cloud masks. The largest hurdle in the processing of the AVIRIS scenes of the 2001 data set was the presence of great amounts of sun glint. This sun glint had a detrimental effect on the AOD retrieval from these scenes. A simple comparison of obviously sun glint contaminated pixels to obviously non-sun-glint contaminated pixels revealed that a threshold mask similar to the reflectance limit land mask could be employed to avoid inclusion of these contaminated pixels.

Figure 12 shows the average spectrum for 10 obviously high sun glint pixels and how it compares with the average spectrum of 10 low sun glint pixels. This comparison revealed a significant difference in the 1562 nm wavelength band. This wavelength was chosen since it is in the region where water-leaving radiance is at a minimum (dark water assumption). Also, there is about a 100% difference between the high glint and non glint pixel at 1562 nm compared to only about a 50% difference in the other two visible peaks at 1000 nm and between 1182 nm and 1293 nm. This difference was exploited to determine a useful sun glint mask for the entire 2001 data set. This sun glint mask allowed the non sun glint pixels in the AVIRIS images to be analyzed between the pixels contaminated with sun glint. Without the use of this mask, the 2001 data set would have been unusable for reliable AOD retrieval.

Sun glint was very prevalent in the 2001 data set. Two to five small Regions Of Interest (ROI's) were selected for each scene. The ROI's were chosen as follows: one

ROI was selected in an area of high sun glint while a second ROI was chosen in an area of relatively low sun glint. The above radiance limit masked an average of approximately 45% of the pixels in ROI's selected for high sun glint ROI's. ROI's selected for slight sun glint had less than 5% of the pixels masked out. In other scenes, ROI's were chosen based on the presence of sediment or other surface features.

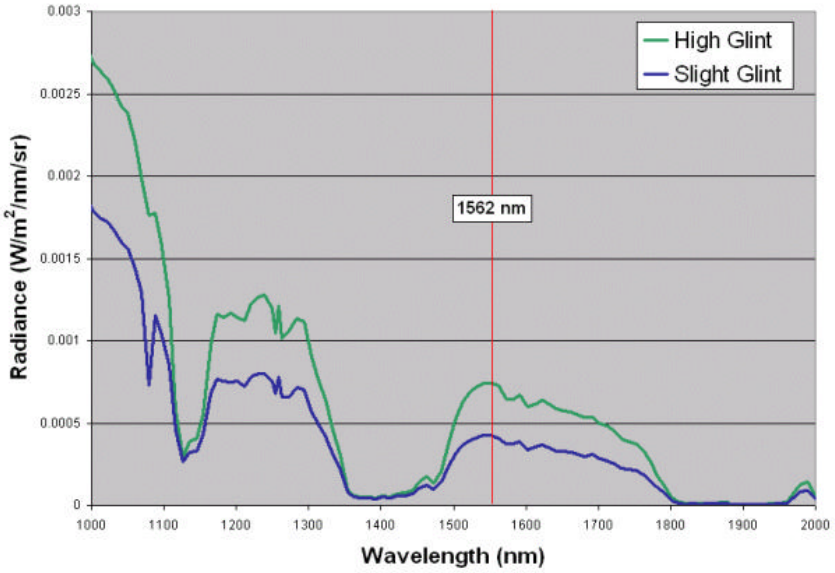

Figure 12 Sun Glint pixels vs. Non Sun Glint pixels

2. Tafkaa

Tafkaa was run on each scene with three wavelength sets chosen for AOD retrieval as described in section IIA. The combinations were chosen based on the typical wavelengths used for SeaDAS/SeaWiFS, NRL's standard default settings, and a combination of the two. Table 2 lists the wavelength combinations used in this study.

Tafkaa performs a pixel by pixel matching technique in order to select the best Model/RH pair that represents the received radiance. Figure 13 shows the various models chosen for Scene 4 of the 1998 data (Figure 9) when the NRL AOD wavelengths (B) are chosen for the retrieval.

Figure 14 shows the various RH models chosen for Scene 4 of the 1998 data (Figure 9) when the NRL AOD wavelengths (B) are chosen for the retrieval. As can be

seen in figures 13 and 14, the small variations radiance received by AVIRIS is enough to cause the Model/RH selection in Tafkaa to vary on a pixel-by-pixel basis. The variations in Model/RH selection depend on the match between measured spectral radiance and Tafkaa lookup tables for each Model/RH pairing given the solar/view geometry of the scene. Along the top of the scene, Tafkaa consistently selects either Urban or Tropospheric coupled with either 90 or 98% RH. Along the bottom of the scene, Tafkaa chooses Coastal or Coastal-a coupled with 50 or 70% RH. In the center of the scene, just above the cloud band many Model/RH pairs are selected. In this region, the spectral signature measured by AVIRIS does not uniquely match a Model/RH pair. In each ROI, the most common Model/RH pair was used in the analysis.

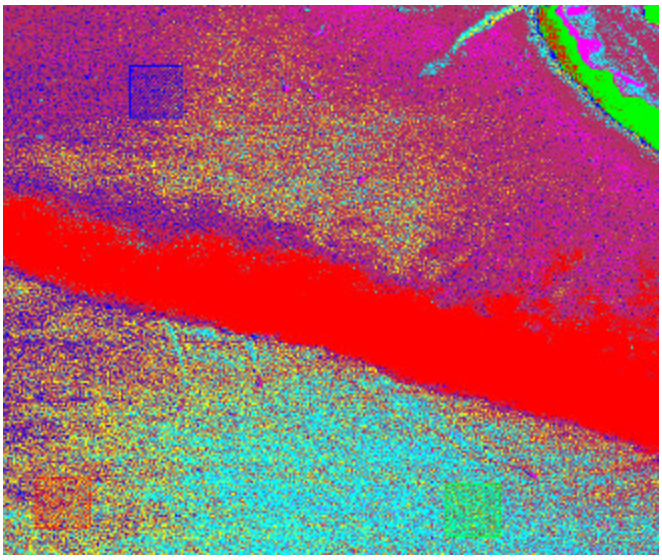

Figure 13. Representation of the models chosen for Scene 4 of the 1998 data set. Red is clouds, Green is the land, Blue is Maritime, Yellow is coastal, Cyan is Coastal-a, Magenta is Tropospheric, and Maroon is Urban.

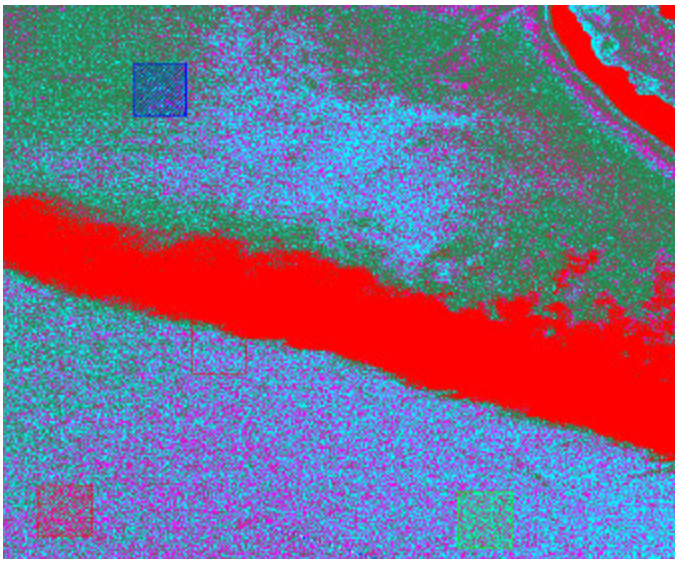

Figure 14 Representation of the RH chosen for Scene 4 of the 1998 data set. Red is clouds and land, Cyan is 50%, Magenta is 70%, Maroon is 80%, and sea green is 90% and 98%.

C. SEAWIFS DATA COLLECTION AND SEADAS EMPLOYMENT

AOD's were retrieved from each of the SeaWiFS data sets utilizing two methods. The first applies the aerosol model developed at the Naval graduate School (NPS) described in Brown (2002). The second used the SeaWiFS Data Analysis System (SeaDAS) software. For each SeaWiFS scene, an RH/model pair was chosen that was either the same as the Tafkaa chosen pair or had a similar size distribution.

THIS PAGE INTENTIONALLY LEFT BLANK

IV. RESULTS

This chapter presents the comparisons of the Tafkaa-retrieved AOD with the SeaDAS-retrieved AOD in two data sets (1998 and 2001). Both data sets provide realistic comparisons between SeaDAS and Tafkaa. The 1998 comparisons provide additional information on the effect of sediment to the Tafkaa atmospheric correction while the 2001 data set provides additional information on the effect of sun glint contamination.

A. 1998 RESULTS

Figure 9 shows the raw image of the scene 4 1998 data set. The use of MASK eliminated the diagonal cloud feature from the image as well as the land located in the upper right corner. The lower left hand region, ROI 1, is in an area where the dark water assumption is most valid.

Figure 15 shows a plot of the spectral variation of the AOD in this region. The solid blue line is the spectral variation of AOD reported by the AERONET sunphotometer located at Brookhaven. The NPS aerosol model was applied to the SeaWiFS data and is identified with a solid yellow line.

The three dashed lines are the spectral variations obtained using Tafkaa on the AVIRIS data. Table 2 lists the various wavelengths chosen in Tafkaa for AOD retrieval. Combination A, 670 nm and 860 nm, compares to the wavelengths used in the SeaDAS AOD retrievals. Combination B is the combination of wavelengths utilized by NRL during ocean color analysis of AVIRIS data. This combination uses wavelengths above 750 nm. Combination C is the NRL combination with the 670 nm wavelength added.

The spectral variations of AOD obtained by forcing SeaDAS to analyze the SeaWiFS data at model/RH combinations that compare to the Tafkaa-selected model/RH pairs are shown in Figure 15 as thin solid lines. Note: The Coastal-a 70 combination was not available for SeaDAS.

The Tafkaa-generated AOD spectral variation curve associated with the modified NRL wavelengths most closely matched the shape of the Brookhaven results. Further, the closest match to the Brookhaven spectral variation curve is the Tafkaa-generated

curve using the modified NRL wavelength combination (A.4.1.C). The SeaDAS-generated curves also matched well to the Brookhaven results. The differences can be attributed to the differences in the spectral fitting procedures of SeaDAS. Also, the day in question is a low optical depth day and the differences in retrieved AOD's may be affected by differences in the radiance measurement errors in the two sensors. The NPS model also provided results that closely matched the Brookhaven sunphotometer.

Particle size plays an important role in radiation-particle interactions. As radiation wavelength increases and interacts with particles of increasing size, the interaction falls into one of three regimes. Particle diameter (2? r) divided by wavelength (*?*) defines the size parameter ($c = 2pr/l$). For solar wavelengths, scatter from cloud droplets and rain is in the largest size category described by geometric scattering. Rayleigh scattering occurs for the smallest particles such as gas molecules. Between these two extremes is the Mie scattering regime that describes scattering by atmospheric aerosols. In this range, particle size and wavelength are roughly equal. Figure 16 shows the Shettle and Fenn (1979) size distributions for the three model/RH pairs selected by Tafkaa for ROI 1. The range of $.1?m$ to $1?m$ is important since this is the range of particle sizes that affect the Mie scattering in the visible portion of the spectrum. In this range, a change in the slope of the size distribution changes the interaction between the incoming solar radiation and the particles. This difference in turn alters slope of the spectral variation of AOD. As shown in figure 16, the Coastal-a/70 curve is steeper than the Maritime/50 curve. Therefore, Tafkaa-generated AOD spectral variation curve for the Coastal-a/70 combination is steeper than the Maritime/50 curve. The SeaDAS spectral variation curves on the other hand perform opposite as expected. As the size distribution flattens from the Coastal/50 to the Maritime/50, the AOD spectral variations derived from SeaDAS should also flatten. The SeaDAS-generated curves get steeper. This is a point for further study and is not addressed in this thesis.

A comparison of ROI 1 with ROI 3, an area of some sediment contamination, provides information on how sediment affects Tafkaa's AOD retrieval. Figure 17 shows a graph of the spectral variation of the AOD for both ROI 1 (dashed curves) and ROI 3 (solid curves). Sediment contributes to the entire spectrum. Water is a strong absorber of

wavelengths greater than 750 nm. Therefore, since the sediment is submerged, the water above the sediment absorbs the radiation above 750 nm. This causes scattering by sediment to contribute more significantly to wavelengths shorter than 750 nm. When Tafkaa analyzes the pixels and performs the spectral matching procedure, this steeper radiance more closely resembles the spectral variation obtained from larger particles. As a result, Tafkaa erroneously selects the Tropospheric and urban models. In this case, Tafkaa chose the urban model with a relative humidity of 98%. This choice in turn caused the spectral variation in the AOD to be steeper than the sediment-free case. It should be noted once again that the modified wavelength combination (A.4.3.c) provided the most accurate results.

B. 2001 RESULTS

Figure 18 shows the raw AVIRIS image of scene 7 from the 2001 data set. The two ROI's described here differ significantly in the amount of sun glint present. ROI 1 lies in an area of high sun glint. Figure 19 shows a graph of the spectral variation of the AOD for ROI 1. The solid lines are the Tafkaa-generated spectral variation in AOD. The dashed lines are the SeaDAS-generated curves. Sun glint contributes to the entire spectrum, as does the sediment described in the previous section. However, since the sun glint is off the surface of the water and therefore, the longer wavelengths are not attenuated by the water, the spectral radiance variation is flatter than if sun glint is not present. Figure 20 shows the elevated values due to sun glint in the region from 1000 nm to 2000 nm. It is this elevation that flattens the spectral variation of AOD retrieval. Therefore, when Tafkaa analyses the pixels and performs the spectral matching procedure, the radiance from the sun glint causes Tafkaa to chose a model/RH pair with a flatter size distribution, Coastal-a/98 for this case, (see Figure 22) leading to flatter variations in AOD than observed at the GISS sunphotometer location

The lower right region, ROI 2, is in an area with reduced sun glint and, therefore, the dark water assumption is more valid than in ROI 1. (See section II.A.) Figure 21 shows a graph of the spectral variation of the AOD in this region. Here again it is interesting to see how Tafkaa behaves where the dark water assumption is valid. See table 2 for the wavelengths in each combination. In this region, it is noted that the curves

match the GISS sunphotometer curve more closely than in the high sun glint region, although they are still flatter than the AOD variation obtained from the GISS site. With a better sun glint mask, results that more closely match the GISS sunphotometer could be obtained. The modified NRL combination (combination C) generated the curve (A.7.2.C) that most closely matches the GISS AOD spectral variation curve.

For this scene, the NPS model did not follow any of the other methods used. More analysis of the NPS model's performance is needed to determine the cause of this significant difference.

Figure 11 shows the raw AVIRIS image of scene 11 of the 2001 data set. As with scene 7 described earlier, the two ROI's described here differ significantly in the amount of sun glint present. ROI 1 lies in an area of high sun glint. Figure 23 is a graph of the spectral variation of the AOD for ROI 1. The dashed lines are the Tafkaa-generated spectral variation in AOD. The solid lines are the SeaDAS-generated curves. Here as in scene 7, the radiance spectrum is flattened by the sun glint contamination. Therefore, Tafkaa chooses a flatter size distribution that results in an AOD spectral variation that is flatter than GISS sunphotometer result.

The reduced sun glint of ROI 2 makes the dark water assumption more valid than in ROI 1. Figure 24 is a graph of the spectral variation of the AOD in this region. Here again it is interesting to see how Tafkaa behaves in this dark-water area. In this region, note that the curves are still flatter than the non sun glint curves obtained from the GISS site. They do show a larger spectral variation than the high sun glint areas. All the Tafkaa-generated curves more closely match the GISS AOD spectral variation curve than does the SeaDAS curve.

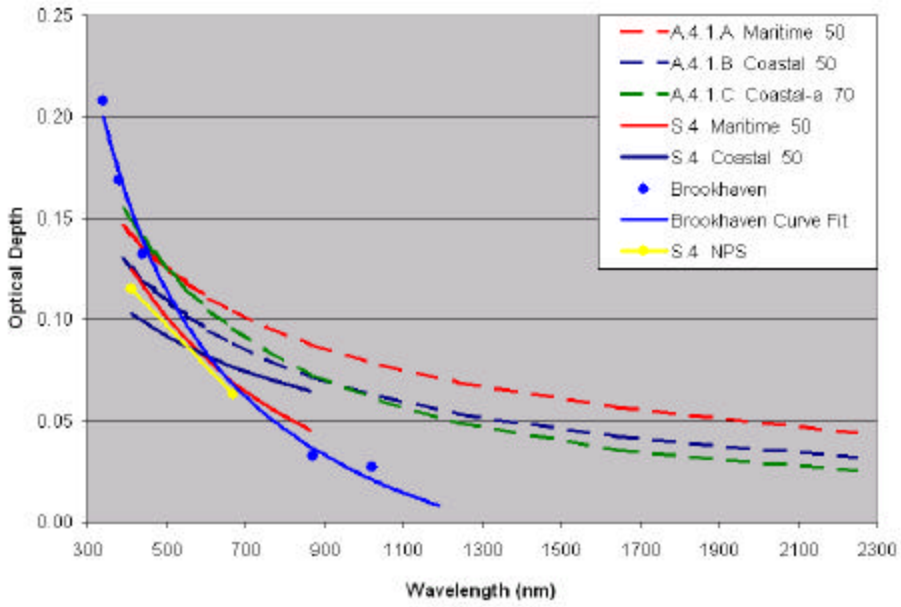

Figure 15. AOD spectral variation in ROI 1 scene 4 of the 1998 data. Dashed lines are AVIRIS/Tafkaa-generated. Solid lines are SeaWiFS/SeaDAS-generated. The blue line is a curve fit of the Brookhaven sun photometer data. The yellow line is SeaWiFS/NPS model-derived.

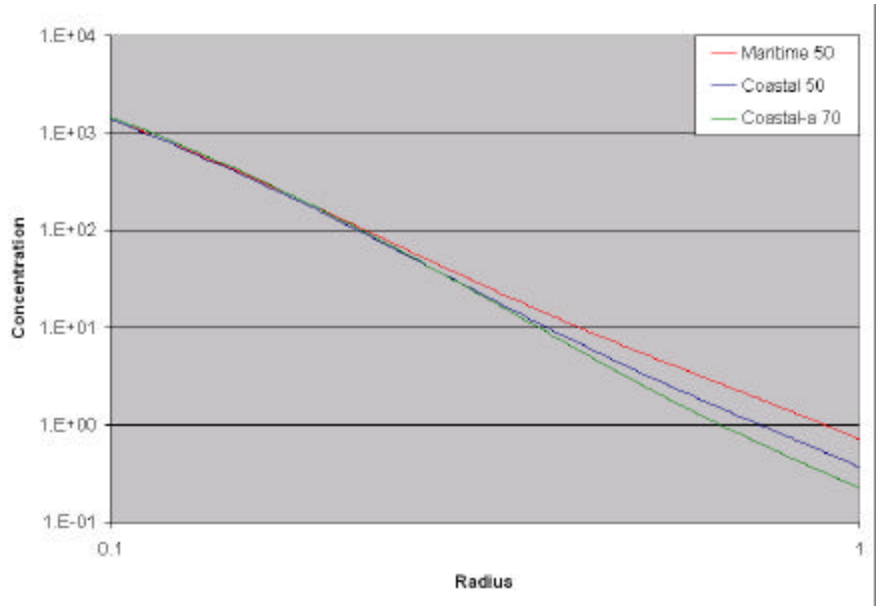

Figure 16. Shettle and Fenn size distributions depicting: Maritime 50, Coastal 50, and Coastal-a 70.

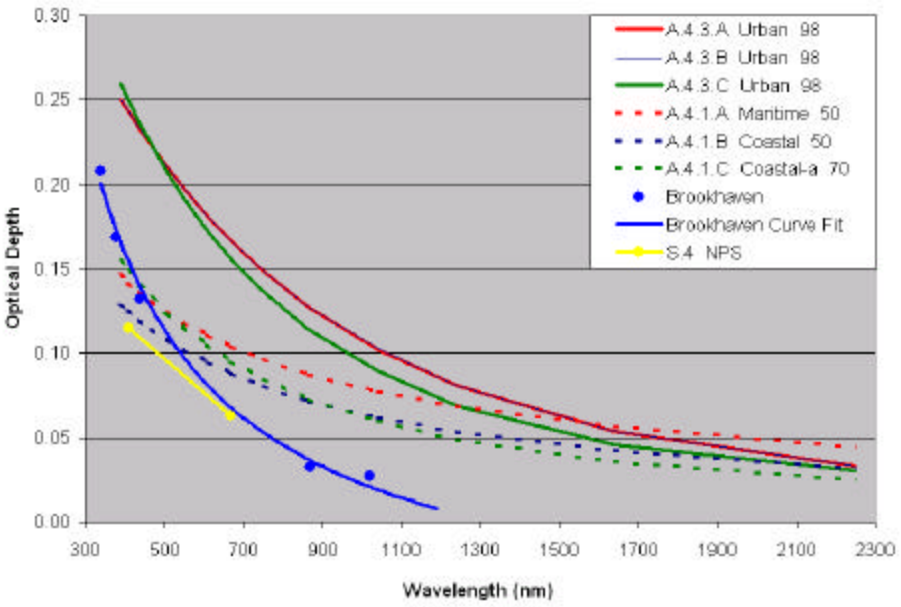

Figure 17. AOD spectral variation in ROI 1 and ROI 3 of 1998 scene 4. Dashed lines are the sediment-free region. Solid lines are for the sediment-contaminated region. The blue line is a curve fit of the Brookhaven sun photometer. The yellow line is SeaWiFS/NPS model-derived.

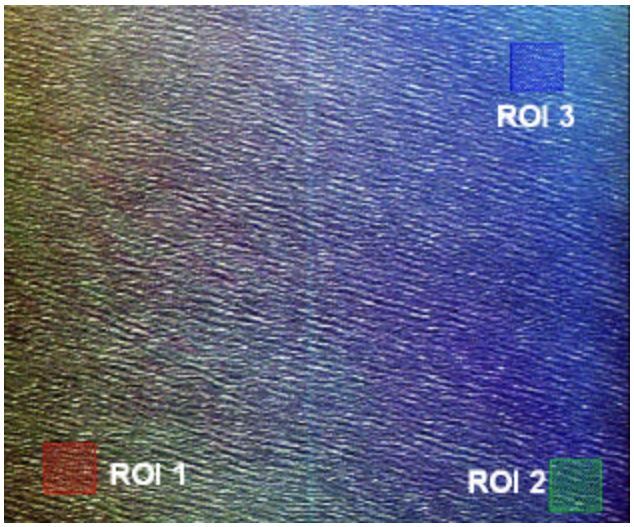

Figure 18. AVIRIS data collected at the LEO site on July 31, 2001. This is scene 7 of the complete data set.

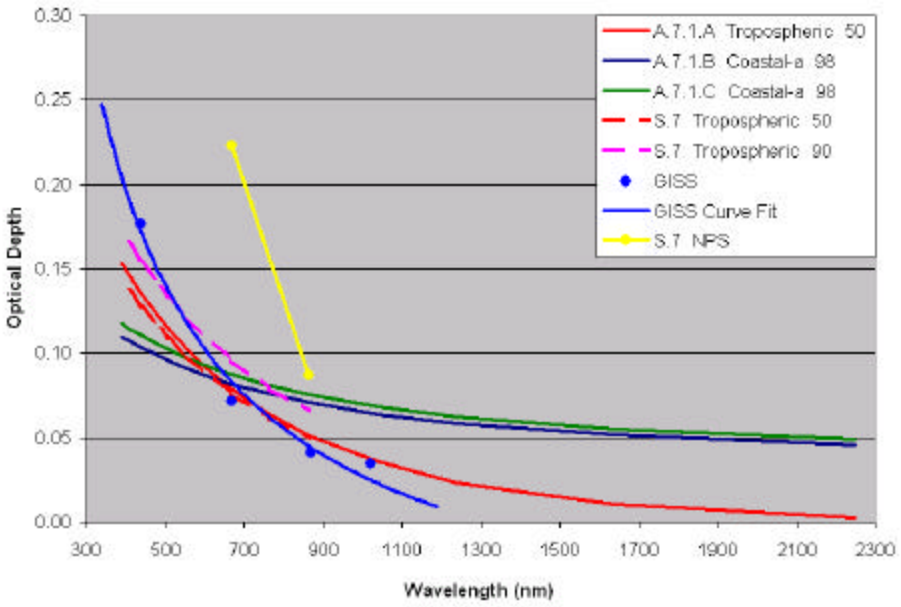

Figure 19. AOD spectral variation in ROI 1 scene 7 of the 2001 data. Solid lines are AVIRIS/Tafkaa-generated. Dashed lines are SeaWiFS/SeaDAS-generated curves. The blue line is a curve fit of the GISS sun photometer data. The yellow line is SeaWiFS/NPS model-derived.

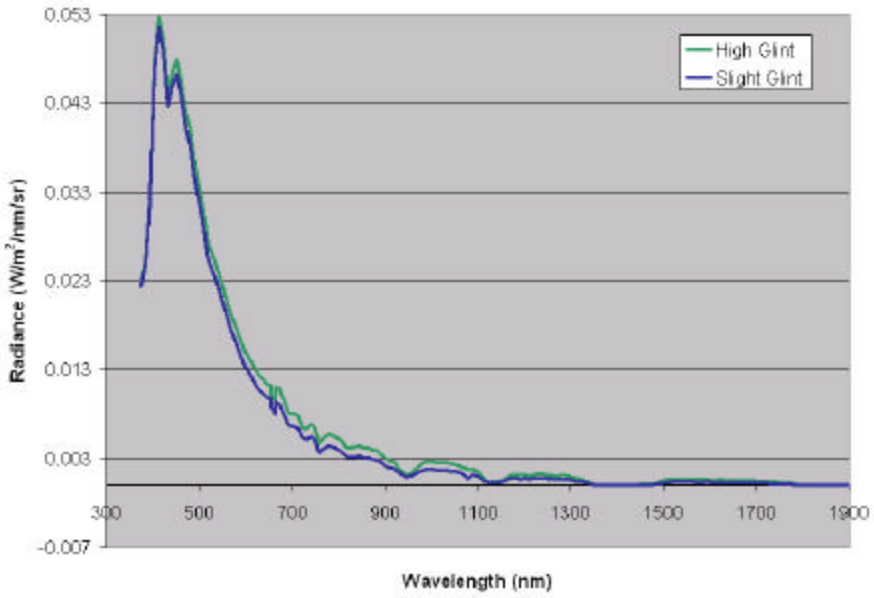

Figure 20. AVIRIS measured radiance for high sun glint pixels and slight sun glint pixels.

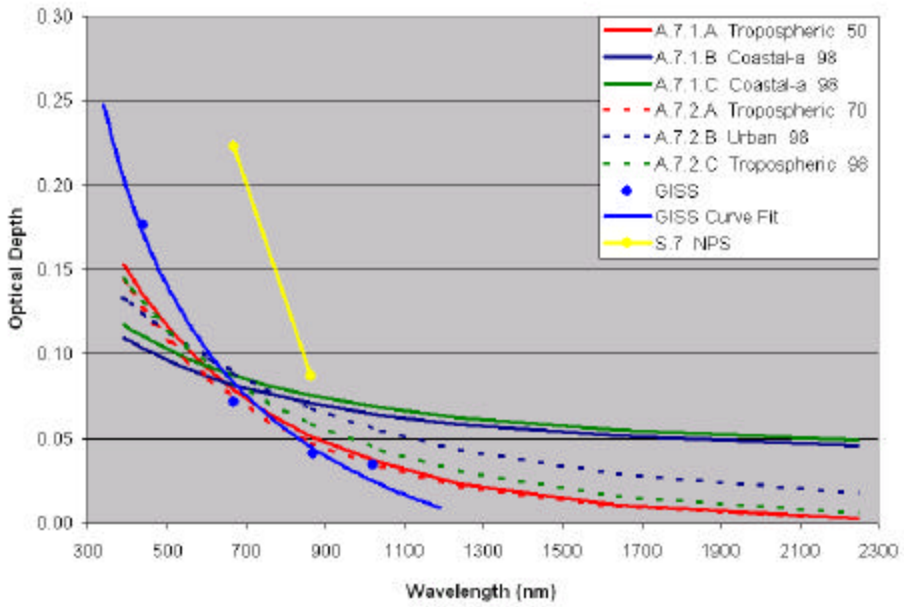

Figure 21. AOD spectral variation in ROI 1 and ROI 2 of scene 7 of the 2001 data set. Dashed lines are from the low sun glint region. Solid lines are for the high sun glint region. The blue line is the GISS sun photometer. The yellow line is SeaWiFS/NPS model-derived.

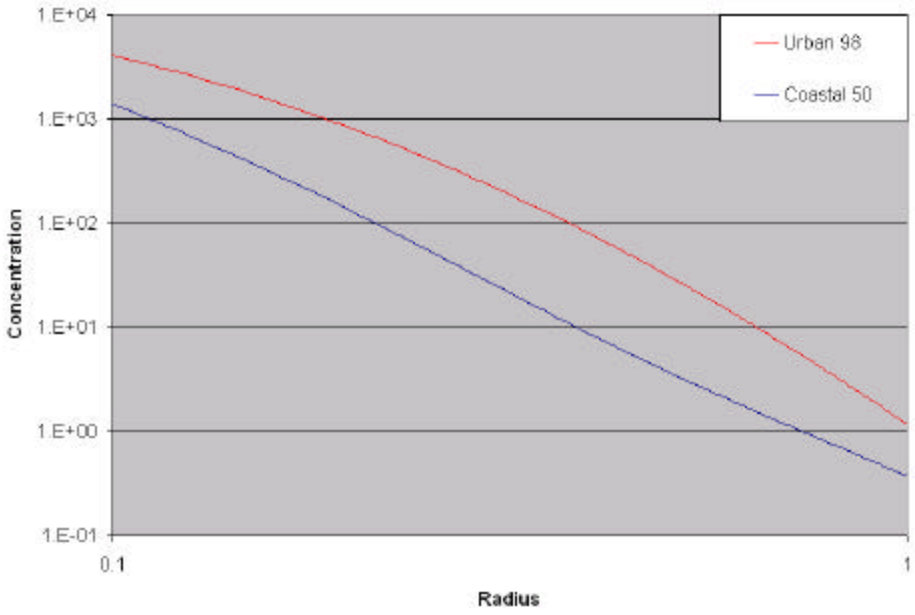

Figure 22. Shettle and Fenn size distributions depicting: Urban 98 and Coastal 50.

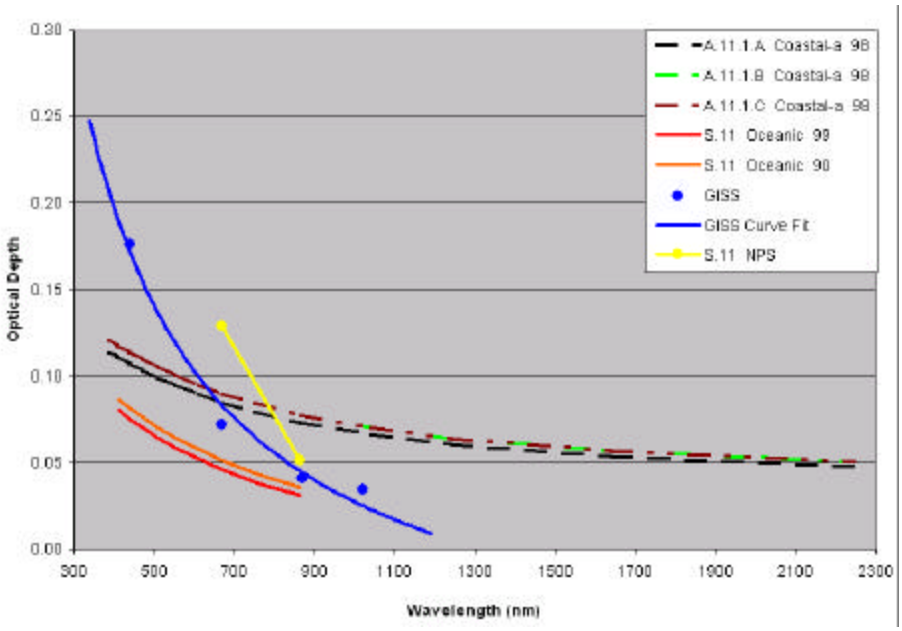

Figure 23. AOD spectral variation in ROI 1 scene 11 of the 2001 data. Dashed lines are AVIRIS/Tafkaa-generated. Solid lines are SeaWiFS/SeaDAS-generated curves. The blue line is a curve fit of the GISS sun photometer data. The yellow line is SeaWiFS/NPS model-derived.

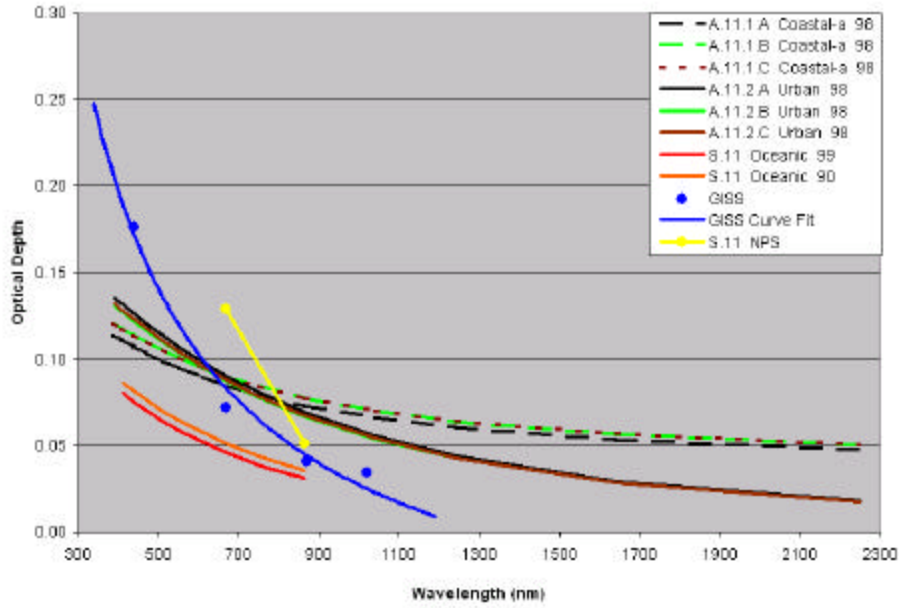

Figure 24. Same as figure 23 with solid lines are for the low sun glint region added.

THIS PAGE INTENTIONALLY LEFT BLANK

V. CONCLUSIONS AND RECOMMENDATIONS

A. CONCLUSIONS

Tafkaa, an algorithm designed by NRL in order to atmospherically correct hyperspectral images was studied and the Tafkaa retrieved aerosol optical depth (AOD) was compared to SeaDAS-retrieved AOD values collected over the LEO site on two separate dates, July 12, 1998 and July 31, 2001. SeaWiFS AOD values were also obtained by using the NPS model on the retrieved SeaWiFS data for validation of the NPS model. Two sunphotometers were used for comparison and minimal ground truthing. There was good agreement between the AOD retrieved from the AVIRIS data by Tafkaa, the SeaDAS-retrieved AOD from the SeaWiFS data, and the AOD retrieved from the sunphotometer data in regions where the dark water assumption was valid.

In areas where the dark water assumption was violated, the expanded wavelengths available to Tafkaa allows for AOD retrievals to match the sunphotometer acquired AOD. Sediments affect the shorter wavelengths, creating a steeper spectral variation of AOD. Tafkaa, with the "SeaWiFS-like" AOD retrieval wavelength combination, performs the best in areas of high sun glint. Longer wavelengths used for AOD retrieval, in the presence of sun glint, raises and flattens the results.

B. RECOMMENDATIONS

As a result of this study, the following recommendations are suggested:

- Continue satellite retrieval validation with additional quality controlled data. The selection of AVIRIS and SeaWiFS data sets that are closer matched in time as well as sets with sunphotometer data available closer to the analyzed regions will also contribute to more substantial results.

- Study the methodology of the SeaDAS program to gain a better understanding of the mechanisms involved in the AOD retrieval from SeaWiFS data.

- Develop a more substantial sun glint mask in order to avoid the flattening of the AOD spectral variation curves in sun glint regions.

- Update the NPS model so it can be applied to hyperspectral imagery.

By following the recommendations of this thesis, the Navy will acquire a better understanding of the optical properties of the atmosphere that have a detrimental effect on electromagnetic observing systems. Hyperspectral imaging is the cutting edge of technology for remote sensing and as such, all the advantages provided by the increased amount and quality of data must be exploited.

LIST OF REFERENCES

Ahmad, Z. and Fraser, R. S. (1982) An iterative radiative transfer code for ocean. Journal of Atmospheric Sciences 37, 656-665.

AVIRIS (Airborne Visible/Infrared Imaging Spectrometer) http://popo.jpl.nasa.gov/html/aviris.cube.html

Brown, B. A. (2002). Aerosol optical depth retrieval by NPS model modified for SeaWiFS input. M.S. Thesis, Naval Postgraduate School, Monterey, CA.

Charlson, R. J., S. E. Swartz, J. M. Hales, R. D. Cees, J. A. Coakley Jr., J. E. Hansen, and D. J. Hoffman (1992). Climate Forcing by anthropogenic aerosols. *Science* **255,** 423-430.

Gao, B. -C, M. J. Montes, Z. Ahmad, and C.O. Davis (2000) Atmospheric correction algorithm for hyperspectral remote sensing of the ocean color from space. *Applied Optics,* Vol. 39, No. 6, 887-896

Intergovernmental Panel on Climate Change (IPCC) (1996). Climate Change 1995, J. T. Houghton et al. (Eds.). Cambridge University Press, New York.

Liou, K. B. (1980). An Introduction to Atmospheric Radiation. Academic Press, New York, 392pp.

Montes, M. A. (2001) Mask users guide16 pp.

Montes, M. A. (2002) Tafkaa users guide 30 pp.

Porter, W. M. and H. T. Enmark (1987) A system overview of the Airborne Visible/Infrared Imaging Spectrometer (AVIRIS)

SeaWiFS (Sea-viewing Wide Field of view Sensor) http://www.sat.Dundee.ac.uk/seawifs.html

SeaDAS (SeaWiFS Data Analysis System) http://seadas.gsfc.nasa.gov/

Shettle E. P., and R. W. Fenn (1979). Models for the aerosols of the lower atmosphere and the effects of humidity variations on their optical properties. AFGL-TR-79-0214 Air Force Geophysics Laboratories, Hanscom AFB, MA.

Smith, P. J. (1998). Remote measurement of aerosol optical properties using the NOAA POES AVHRR during ACE-1, TARAFOX, and ACE-2. M.S. Thesis, Naval Postgraduate School, Monterey, CA.

INITIAL DISTRIBUTION LIST

1. Defense Technical Information Center
   Ft. Belvoir, Virginia 22060-6218

2. Dudley Knox Library
   Naval Postgraduate School
   Monterey, California

3. Chairman, Code MR
   Department of Meteorology
   Naval Postgraduate School
   Monterey, California

4. Professor Philip A. Durkee
   Department of Meteorology
   Naval Postgraduate School
   Monterey, California

5. LCDR James O. Rasure
   Department of Meteorology
   Naval Postgraduate School
   Monterey, California